ELSEVIER

Journal of Fluids and Structures 20 (2005) 467–482

JOURNAL OF FLUIDS AND STRUCTURES

www.elsevier.com/locate/jfs

The contrast in phase angles between forced and self-excited oscillations of a circular cylinder

H. Al Jamal, C. Dalton*

Department of Mechanical Engineering, University of Houston, Houston, TX 77204-4006, USA

Received 4 October 2004; accepted 23 February 2005
Available online 12 May 2005

Abstract

The problem of vortex-induced vibration (VIV) on a circular cylinder has historically been considered from the viewpoints of both self-excited and forced oscillations. In an intermediate Reynolds number range, the self-excited case typically has an irregular displacement response that occurs without a constant amplitude or frequency. In a forced oscillation of constant amplitude and frequency in this intermediate range, the applied force can either lead or lag the cylinder oscillation with a constant phase angle. In a self-excited oscillation, the phase angle could possibly vary a great deal because of a more irregular oscillation. This study presents a set of phase angles determined from 2-D CFD/LES calculations of the self-excited oscillations of a cylinder at Re = 8000 over a range of lock-on conditions. The results show that the phase angles determined from the self-excited case do not have a consistent trend but behave in an irregular manner, not at all like those in a forced sinusoidal oscillation. Both a spectral analysis and a complex demodulation analysis of the displacement and lift coefficient confirm that this self-excited behavior does not occur at a single frequency or at a constant phase angle at the Reynolds number for this study.

1. Introduction

Vortex-induced vibration (VIV) caused by a fluid flowing past a bluff body has been a subject of interest to structural engineers and fluid mechanicians for years. Numerous experimental studies have been conducted on this self-excited oscillatory response of a bluff body to the shedding of vortices. The vibratory response occurs as the shedding frequency approaches the natural frequency of the structural member, i.e., the bluff body. When the natural frequency and the vortex shedding frequency are approximately the same (within $\pm 10\%$), the vortex shedding frequency connects to the natural frequency (or an approximation of it) and remains at that value for an appreciable increase in fluid velocity. During this connected period, the cylinder can vibrate at noticeable amplitudes.

The equation of motion representing the transverse (only) motion of a cylinder in a uniform approach flow is generally expressed as

$$my'' + cy' + ky = F_L(t), \tag{1}$$

where y is the transverse displacement, m is the structural mass (no added mass effects are included in m), c is the structural (or material) damping, k is the transverse structural stiffness, and $F_L(t)$ is the fluid-forcing function, per unit

*Corresponding author.
E-mail address: dalton@uh.edu (C. Dalton).

0889-9746/$ - see front matter
doi:10.1016/j.jfluidstructs.2005.02.001

length of the cylinder, in the y (transverse) direction, initiating the cylinder response. The primes indicate the derivatives with respect to the dimensional time t. The nondimensional form of Eq. (1) is

$$\ddot{Y} + \zeta(4\pi f_{\text{vac}})\dot{Y} + (2\pi f_{\text{vac}})^2 Y = \frac{C_L(\tau)}{m^*\pi}, \tag{2}$$

where $Y = y/R$, $\tau = U_o t/R$, m^* is the ratio of the effective cylinder density to the fluid density, i.e., the mass factor, $f_{\text{vac}} = (f^d_{\text{vac}} R)/U_o$ is the cylinder nondimensional natural frequency in a vacuum with f^d_{vac} as the corresponding dimensional natural frequency, ζ is the structural damping factor and $C_L(\tau) = F_L(t)/RU_o^2$. The dots indicate the derivatives with respect to the nondimensional time τ.

It is Eq. (1) or (2) that must be solved to determine the cylinder displacement in a self-excited oscillation. When the motion is a forced oscillation, then the cylinder inertia force must be subtracted from the $F_L(t)$ term in Eq. (1). When the motion is self-excited, then the added mass is not a factor and the $C_L(\tau)$ term in Eq. (2) is represented independently of the added mass. If $C_L(\tau)$ is measured, then it must be, by definition, compatible with the calculated and/or measured cylinder displacement from Eqs. (1) or (2). The added mass term is not represented explicitly when $C_L(\tau)$ is determined using the calculated pressure and shear stress distributions on the cylinder because the fluid force term $C_L(\tau)$ (or $F_L(t)$) contains the added-mass effects implicitly. When $C_L(\tau)$ is calculated, it is determined by solving the governing fluid flow equations, subject to whatever wake turbulence model is used, for sufficiently large Reynolds numbers.

There is certainly the possibility of a phase angle between the fluid forcing function and the displacement of the cylinder. The value of the phase angle would depend on whether the self-excited oscillation is periodic with constant amplitude or is an irregular motion, i.e., neither constant period nor amplitude. Both situations have been observed experimentally and computationally. It is not yet clear what the factors are that produce one situation over the other.

In constant-amplitude, forced-oscillation investigations, it has been observed from many studies that the sinusoidal oscillation trails the force by a constant phase angle. A reasonable approximation to the dimensional force and the response is given by

$$y(t) = A_o \sin \omega_{\text{ex}} t, \tag{3}$$

$$F_L(t) = F_o \sin(\omega_{\text{ex}} t + \phi), \tag{4}$$

where A_o is the amplitude of oscillation, F_o is the force amplitude, ω_{ex} is the excitation frequency, and ϕ is the phase angle. The measurement of the fluid driving force is relatively easy in the forced-oscillation problem and the actual force on the cylinder; i.e., the applied force by the flow field, is obtained by subtracting the inertia force of the cylinder, as a result of the added mass, from the measured force that contains the forces from the flow stresses and the added mass. The oscillation amplitude in these forced-oscillation studies is typically sinusoidal with a fixed amplitude and a prescribed frequency. In this form of cylinder oscillation, the phase angle has typically been found to be approximately 0° or 180° depending on the physical parameters which control the vortex modes. The reason for this change in phase angle is due to a change in the mode of vortex shedding, as first noted by Zdravkovich (1982). This change is called vortex switching and has been observed experimentally by Gu et al. (1994) and numerically by Lu and Dalton (1996).

1.1. Forced oscillations

In the early days of studying VIV, it was felt that an understanding of the forced-oscillation problem would lead to an understanding of self-excited oscillations. We now know that this reasoning is not strictly correct. However, studies of the forced-oscillation problem have helped to develop an understanding of self-excited oscillations and the forced-oscillation problem is still quite interesting in its own right. Early investigations of the forced-oscillation problem were by Bishop and Hassan (1964), Lienhard and Liu (1967) and Sarpkaya (1978), and more recently by Tutar and Holdo (2000) and Carberry et al. (2001), among others. Bishop and Hassan (1964) did the first experiments on a cylinder in forced oscillation. They identified two critical frequencies that provided the bounds for the vortex-switching phenomenon to occur. Within this frequency range, the vortex formation switched from one side of the cylinder to the other, which results in a phase angle change from 0° to 180°.

Sarpkaya (1978) also conducted an experimental investigation of the forced-oscillation case. His purpose was to study the in-phase and out-of phase components of the time-dependent force and then to use these force components to predict the dynamic response of the cylinder undergoing forced oscillation. Sarpkaya represented the transverse force in the Morison equation style, decomposing the measured transverse force in terms of drag (C_{DL}) and inertia (C_{ML}) coefficients. He found a sharp decrease in the value of C_{ML} at $V_R = 5.1$ in a plot of A/D versus V_R (the reduced velocity, $V_R = U_o/2Rf_{\text{ex}}$); this shows clearly that a change in the wake-vortex structure has occurred. (In the definition of V_R, U_o is the approach velocity, R is the cylinder radius, and f_{ex} is the oscillatory frequency, $f_{\text{ex}} = \omega_{\text{ex}}/2\pi$.) This change leads to a negative value of C_{ML} for all A/D values beginning at $V_R = 5.1$. The drag coefficient for the transverse motion also has a range of negative values, which implies that the cylinder is gaining energy from the fluid in this range; these negative values of C_{DL} infer synchronization.

The forced-oscillation study of Tutar and Holdo (2000) was a 3-D CFD/LES representation. They did extensive calculations at $\mathrm{Re} = 2.4 \times 10^4$ and $A/D = 0.11$ (a relatively small oscillation). Tutar and Holdo did not address the phase-angle problem, but presented their results at four different values of V_R and for both 2-D and 3-D cases. They provided vorticity–contour comparisons at the different reduced velocities which showed a dependence of the contours on the value of V_R. The 3-D calculations were noted to agree more closely to the experimental results, as expected.

Carberry et al. (2001) also examined the forced-oscillation problem experimentally, subject to the phase-angle behavior described in Eqs. (3) and (4). In particular, they looked at the effect of the frequency ratio f_{St}/f_{ex} on the phase angle. They found that an increase in oscillatory frequency (or a decrease in vortex-shedding frequency) over a fairly narrow range could cause a fairly sudden decrease in phase angle from a mean value of approximately 160° to a mean of approximately 0°. As the phase angle changed, the magnitude of the lift coefficient increased suddenly from about 0.2 to 1.0. These lift-coefficient and phase-angle values had a consistent behavior with slight fluctuations about almost constant values; they are given here as approximate values from Carberry et al.

Another forced-oscillation CFD study was conducted by Guilmineau and Queutey (2002). They considered a transversely oscillating cylinder at $\mathrm{Re} = 185$ with $0.8 < (f_{St}/f_{ex}) < 1.2$ and $A/D = 0.2$ which is a relatively small amplitude of oscillation. As f_{St}/f_{ex} increased within the specified range, the wake vortex structure became closer to the cylinder and a limiting position was reached at which time the phenomenon of vortex switching occurred. This is consistent with the experimental results of Gu et al. (1994) and the computational results of Lu and Dalton (1996).

Note that the changes in the reduced velocity (V_R) in the forced-oscillation cases just discussed are caused by increasing approach velocity (U_o) of the fluid, not by decreasing the excitation frequency (f_{ex}). This method of changing V_R introduces an unaccounted-for Reynolds number effect into the results.

To emphasize an earlier comment, the phase angles in the forced-oscillation studies presented herein are noted to be approximately 0° or 180° depending on the physical parameters which control the vortex modes. The reason for the change in phase angle is due to a change in the mode of vortex shedding.

1.2. Self-excited oscillations

In the self-excited case, the cylinder displacement is not controlled externally. The cylinder is free to respond to the time-dependent force on the cylinder. If we restrict the vibratory response to the transverse direction, then it is the lift (or transverse force) to which the cylinder responds. In the computational approach (CFD) to solving the self-excited oscillation (VIV) problem, the issue is to determine the forcing function on the right-hand side of Eq. (1). This is done by solving the Navier–Stokes equations, subject to whatever turbulence model is used. At each time increment of the CFD solution, Eq. (1) is solved to obtain the cylinder response. The boundary conditions of the Navier–Stokes equations are then updated because the cylinder is now moving and the forcing function is found at the next time level. This process continues ad infinitum. In the experimental approach to the self-excited VIV problem, the approach velocity is increased incrementally, causing V_R to increase which, in turn, causes the cylinder to vibrate when $f_{St}/f_{vac} \rightarrow 1$, where f_{St} is the vortex shedding frequency of the stationary cylinder and f_{vac} is the natural frequency in a vacuum. Again, this technique introduces a Reynolds number effect into the results.

Feng (1968), in one of the very first VIV investigations, considered a circular cylinder in a free vibration in a wind tunnel, a situation which yielded a large value of m^*, leading to a relatively high value of $m^*\zeta$ (called the mass-damping term). He examined the effect of the phase angle as defined from Eqs. (3) and (4). Feng did not measure the force but used the pressure at the stagnation point of the moving cylinder, i.e., $\pm 90°$ from the approach flow stagnation point on a cylinder at rest, to relate to the displacement. This concept is equivalent to the transverse force and its relationship to the displacement. Feng found a trend in the phase angle as his "magnetic damping" increased. At low damping, he found an overall, but not quite linear, increase of phase angle with increase in reduced velocity. At the lowest value of magnetic damping, Feng found that the phase angle increased from 0° to 55° as the reduced velocity increased from 0.8 to 0.98. As the magnetic damping increased, the phase angle leveled off to a more-or-less constant value at 0°.

Moe and Wu (1990) examined both the forced oscillation and self-excited cases in both one and two degrees of freedom. They found several significant results: (i) the lock-on range was similar for both free (self-excited) and forced vibrations; (ii) the lift force was irregular for both cases, especially so for the free vibration case; (iii) the range of V_R for lock-on is greater if the cylinder is allowed to vibrate in both transverse and in-line directions, i.e., two degrees of freedom. Moe and Wu also found that the phase angle was influenced by small changes in the reduced velocity for in-line oscillations. At $V_R = 5.51$, Moe and Wu found that the phase angle is 180°, while, at $V_R = 5.93$, the in-line self-excited oscillation has a phase angle of 0°, while the forced-oscillation case has a phase angle of 180°. However, the in-line oscillations are not expected to follow the same trends as the transverse oscillations due to a different influence of the oscillations on the wake structure. And, in fact, they do not, with the maximum in-line oscillations occurring at different values of V_R than for the transverse oscillations.

Brika and Laneville (1993) also presented experimental results for VIV of a cable. Their phase angles are not identified numerically, but they do show sharp abrupt jumps, apparently when the mode behavior switches from the initial branch to the lower branch. Brika and Laneville show flow-visualization results for two cases: for amplitude-to-diameter (A/D) ratios of 0.27 and 0.4, both at $V_R = 5.84$ and $\mathrm{Re} = 7350$. They observed a 2S mode for $A/D = 0.27$ and a 2P mode for $A/D = 0.4$. This does not agree exactly with the Williamson and Roshko (1988) forced-oscillation map which suggests that the 2P mode is the shedding mode for both cases. However, the Reynolds number ($\mathrm{Re} = 7350$) for the Brika and Laneville results is notably higher than that on which the Williamson and Roshko map is based. The larger value of Re is perhaps the explanation for the difference between the Brika and Laneville result and the Williamson and Roshko map. The hysteresis effect shown in the A/D versus V_R plot is closely related to the 2P to 2S jump as suggested by Sarpkaya (2004) who noted that the 2S mode is the most robust of the known modes while the 2P mode is perhaps the most precarious. In this context, the term 2S means that two single vortices of opposite sign are shed per cycle; the term 2P means that two pairs of vortices of opposite sign are shed per cycle; and P+S means two vortices of opposite sign plus a single vortex are shed per cycle.

Moe et al. (1994) conducted a two degree of freedom experiment on a self-excited oscillation at both subcritical and critical values of Re. They found considerable in-line motion accompanying the dominant transverse motion with the latter different from the transverse-oscillation only case. For the subcritical value of Re, the drag coefficient was observed to increase on the order of 200–300% compared to the fixed-cylinder result. Conversely, the drag coefficient for the critical case increased to about 80% greater than the fixed-cylinder result at the same value of Re. However, the magnitude of the transverse oscillation was about one cylinder diameter for the subcritical case and slightly larger for the critical case. The aspect ratio (length to diameter) was 13 for the subcritical case and 15.6 for the critical case. Moe et al. did not discuss the lift coefficient and its variation.

Sarpkaya (1995) also examined both free and forced vibrations, allowing both transverse and in-line oscillations to occur in the free-vibration case. He found that the two degree of freedom response in free oscillations produced about a 20% larger range of $f_{\mathrm{St}}/f_{\mathrm{ex}}$ $(= V_R St)$ when the natural frequency was the same in both transverse and in-line directions. This particular result was obtained at $\mathrm{Re} = 3.5 \times 10^4$ which is considerably higher than most of the experimental studies that are cited herein.

More recently, Khalak and Williamson (1999) also studied the self-excited oscillation problem and assumed that the displacement and force were described by Eqs. (3) and (4). A brief summary of their results is that they found two relatively constant phase angles, 0° and 180°, to represent the relationship expressed in Eqs. (3) and (4). This change in phase angle is attributed solely to the response jumping between the upper and lower branches of the amplitude/reduced-velocity plot, which apparently is also related to vortex switching as discussed earlier.

In the self-excited vibration problem, simultaneous measurement of force, displacement, and vorticity is relatively difficult and has been accomplished only recently by Govardhan and Williamson (2000). They assumed that the force and displacement were out of phase as described by Eqs. (3) and (4). Their measurements yielded results consistent with the assumption suggested by these two equations. Govardhan and Williamson found a phase angle behavior related to the initial, upper, and lower branch descriptions of the self-excited cylinder. For the initial and upper branches (relatively low values of V_R), the phase angle was essentially 0°. For the lower branch (relatively high values of V_R), the phase angle was 180°. The oscillatory response of the cylinder in this self-excited case was sinusoidal (see Fig. 4 therein) which led to the constant phase angle values. Govardhan and Williamson did not show the force measurements but, since the phase angles are essentially constant and the oscillations are sinusoidal, one would expect the transverse force to be sinusoidal also.

Sarpkaya (2004) has suggested that sinusoidal responses in the free-vibration cases occur when Re is relatively low. When the value of Re is sufficiently high, the cylinder response is irregular both in amplitude and period. Al-Jamal and Dalton (2004) have also addressed this issue.

We want to address the question of the behavior of the phase angle in transverse motion VIV. Does this phase angle have the same kind of behavior as in a forced oscillation, i.e., a switch from 0° to 180° as the timing of vortex shedding changes? Does the phase angle have an irregular behavior when the lift coefficient has a nonperiodic, variable-amplitude behavior? If the latter is correct, what are the factors which influence the phase angle? Possibilities include the approach flow Reynolds number, the reduced velocity, the mass factor, the amplitude-to-diameter ratio, and the ratio of the (stationary cylinder) vortex-shedding frequency to the natural frequency of the cylinder in a vacuum. The scope of these possibilities is greater than we can address based on the information available to us at this point. The full response to these questions remains for further investigation.

To complicate the situation, investigators have found that both phase angle behaviors exist. First, we look at those VIV studies which have produced a phase angle which was either 0° or 180° (approximately in each case). Khalak and Williamson (1999) found that the phase angle on the lower branch (relatively high values of V_R) had a reasonably constant value of 0° with occasional positive excursions sometimes reaching 180°. They also found that the upper/lower transition region had phase angle variations that ranged primarily from 0° to 180° with occasional excursions below 0° to 90° and from 180° to 270°. In addition, for the lower branch, the phase angle was found to oscillate from approximately 135° to approximately 225° about a mean value of approximately 180°. Khalak and Williamson showed that the phase angle jump from 0° to 180° occurred with a mode change from 2S to 2P.

In the Khalak and Williamson experimental study, V_R was varied by increasing the velocity which then increased the value of Re. Their lower branch was for $5000 < \mathrm{Re} < 10\,000$ (approximately) and their upper branch was for $4000 < \mathrm{Re} < 7000$ (again approximately). Thus, as noted by Sarpkaya (2004), there was some Reynolds number influence on the results since the location of the transition point in the shear layer has a Reynolds-number dependence for the range of Reynolds numbers studied by Khalak and Williamson.

Govardhan and Williamson (2000) found that the phase angle was essentially 0° for the initial and upper branches and fluctuated about approximately 180° for the lower branch. The fluctuations appear to range from (approximately) 120° to (approximately) 215°. The range of Reynolds numbers in the Govardhan and Williamson study appears to be the same as in the Khalak and Williamson study. The experiments in both studies were conducted by increasing the velocity, hence Re, to increase V_R.

There have been several CFD studies which have examined the VIV problem using DNS or LES or RANS when the Reynolds number was sufficiently high. The computational studies of Karniadakis and his coworkers have made a notable contribution to the DNS calculation of flow past a vibrating cylinder. Evangelinos and Karniadakis (1999) conducted a 3-D DNS study of a cable (tension-dominated) experiencing VIV at $\mathrm{Re} = 1000$. Their phase angles were determined by complex demodulation analysis [see Bloomfield (1976)]. The phase angle behavior had its greatest variation at several axial positions, ranging from approximately −100° to 150°. Evangelinos and Karniadakis found the wake structure to be mixed regarding the 2S, 2P, etc. description of Williamson and Roshko (1988). There was no dominant vortex structure appearing in the wake with a 2P pattern in the near wake followed by a 2S pattern before becoming unstable further downstream. That the vortex structure was variable inferred that it was difficult to determine if the calculated result represented the upper branch or the lower branch.

Blackburn and Henderson (1999) used a spectral element discretization to represent a forced oscillation at A/D for $\mathrm{Re} = 500$. They concentrated on oscillation frequencies near the fixed-cylinder vortex-shedding frequency. The 2S shedding mode was observed for all frequency ratios for which calculations were done; the 2P shedding mode was not observed in this study.

Blackburn et al. (2001) used a spectral element-Fourier spatial discretization method to represent the flow. Their results are apparently for the lower branch at $V_R = 6.3$, but a considerable difference in amplitude response was found between results of 2-D and 3-D calculations. The phase angle was found to vary from approximately 40° to approximately 110° over the range of times shown for the 3-D results. The lift coefficient was approximately periodic with a variation in amplitude but with a reasonably constant frequency. A 2P shedding pattern was observed at $\mathrm{Re} = 556$.

In Al Jamal and Dalton (2004), a 2-D LES calculation was done for the self-excited case at $\mathrm{Re} = 8000$. In the synchronization range, the response of the cylinder was irregular, with the amplitude and phase angle changing from cycle to cycle. The lift coefficient had a significant cyclic dependence in its amplitude, which led to a nonsinusoidal displacement and a nonconstant phase angle. Typical results are shown in Figs. 1 and 2 at $\mathrm{Re} = 8000$, at $f_{\mathrm{vac}} = 0.09$, $\zeta = 0.0$ and $f_{\mathrm{vac}} = 0.12$, $\zeta = 0.02$, respectively. Al Jamal and Dalton did not find the 2S, 2P, etc. patterns in their calculated results, quite likely because of the very irregular displacement response.

Lucor et al. (2004) obtained a DNS solution of a self-excited rigid cylinder at $\mathrm{Re} = 1000$, 2000 and 3000 and presented phase angle results for $V_R = 4.99$ and 6.00. They found considerable variation of the phase angles for these two values of V_R, both of which represent the lower branch of the displacement plot. They found that, at $\mathrm{Re} = 3000$, a wake state existed that was "characteristic of the lower branch response with a 2P shedding mode".

Dong and Karniadakis (2004) obtained a DNS solution for forced oscillation of a cylinder at $\mathrm{Re} = 10{,}000$. They showed a plot of the lift coefficient and displacement curves at $f_o D/U_o = 0.25$, where f_o is the oscillation frequency. The lift and displacement are in phase for this condition with the lift coefficient ranging from a magnitude of approximately 1.4–2.4. At a lower frequency ratio (0.14), the lift and displacement were out of phase by 180°.

Guilmineau and Queutey (2004), in a calculation using a 2-D RANS model for a self-excited oscillation, found that the phase angle had a sharp, abrupt increase from approximately 0° at $V_R = 4$ to approximately 180°. The phase angle then decreased to approximately 160° at $V_R = 7$ and then increased to and leveled off to 180° at a value of V_R of

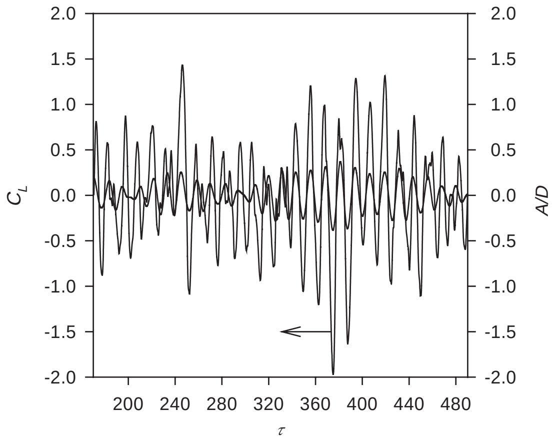

Fig. 1. Lift coefficient and A/D versus time for $V_R = 5.56$ ($f_{\text{vac}} = 0.09$) and $\zeta = 0.0$ for Re = 8000.

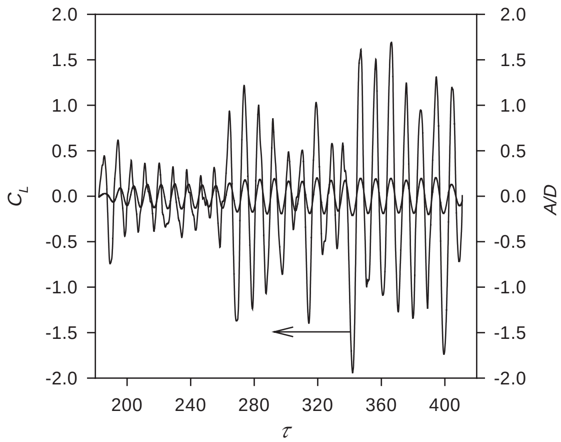

Fig. 2. Lift coefficient and A/D versus time for $V_R = 4.167$ ($f_{\text{vac}} = 0.12$) and $\zeta = 0.02$ for Re = 8000.

approximately 11. The vortex-shedding pattern was observed to be 2S at $V_R = 3.63$, 4.51, and 11.0. At $V_R = 6.91$, the vorticity contours clearly revealed a 2P pattern.

2. Discussion

For the forced-oscillation problem, there seems to be a phase-angle correlation between force and displacement. The phase angle is either 0° or 180° depending on the flow parameters. These results are found in the work of Ongoren and Rockwell (1988), Carberry et al. (2001), and others.

In the discussion that follows, we will use the term phase angle as it is implied for a sinusoidal oscillation. Our phase angle is defined by the difference in time that the displacement follows the forcing function after each zero upcrossing of the forcing function.

For the self-excited problem, the phase angle seems to have either a consistent value or a variable value depending on whether the oscillation is sinusoidal or irregular. Govardhan and Williamson (2000) found a relatively constant phase angle for their sinusoidal oscillation. Blackburn et al. (2001) found a variable phase angle, but did not specify what form the oscillation took. Their lift coefficient seems to be sufficiently variable that their oscillation would not have been expected to be sinusoidal.

The constant phase angle and sinusoidal oscillation seem to have a connection through the vortex-shedding mode descriptions such as the 2S, 2P, etc., modes. When the oscillation is sinusoidal, the vortex structures have repeatability due to the constant-amplitude, constant-period oscillation. That is, the vortex modes are essentially the same from cycle to cycle when none of the physical parameters, such as A/D, f_{St}/f_{vac}, Re, etc., have changed. The repeatability of the cyclic motion leads to the standard vortex modes readily observed in the constant-amplitude forced-oscillation cases.

This situation is different when the self-excited oscillation is not sinusoidal. In this case, neither the amplitude nor the oscillation frequency is constant. Thus, the shear layers and vortex structures never become sufficiently established for periodic conditions to prevail. The implication is that the cylinder amplitude and velocity change from cycle to cycle. This further infers that the time required for repeatable vortex structures probably is not met and these ‘‘expected’’ wake modes (2S, 2P, etc.) are not generated. When the wake structure is not consistent or repeatable, it follows that the phase angles also are not repeatable and are, therefore, not constant.

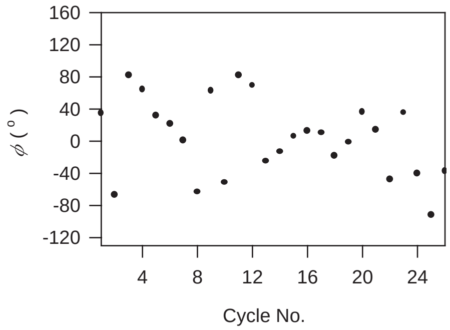

Fig. 3. Phase angles versus cycle number for $f_{vac} = 0.09$ and $\zeta = 0.0$ for Re = 8000.

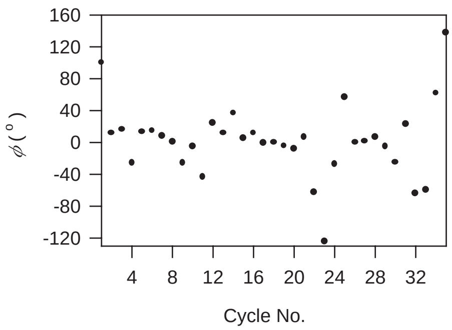

Fig. 4. Phase angles versus cycle number for $f_{vac} = 0.11$ and $\zeta = 0.0$ for Re = 8000.

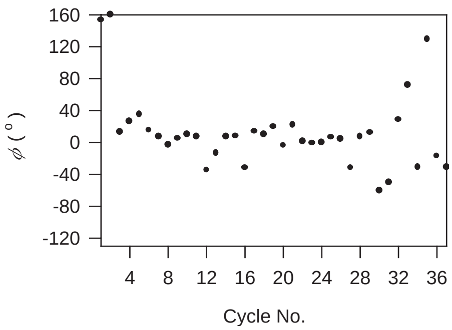

Fig. 5. Phase angles versus cycle number for $f_{vac} = 0.12$ and $\zeta = 0.0$ for Re = 8000.

3. Analysis of the results of Al Jamal and Dalton (2004)

3.1. Phase angles

A random signal, by definition, would typically have many frequencies, each with its own amplitude, contained in the signal. The results to be discussed herein have both the forcing function and the oscillation amplitude as irregular, not random, because of the limited number of frequencies in the signal. Using the definition of a random signal, our results are not random, but irregular, because they have neither a constant amplitude nor a constant frequency. When two signals are irregular, there is no specific trend to the phase angle behavior between the two analyzed signals. This suggests that there is an unpredicted irregularity in both the amplitude and the frequency associated with each signal, in

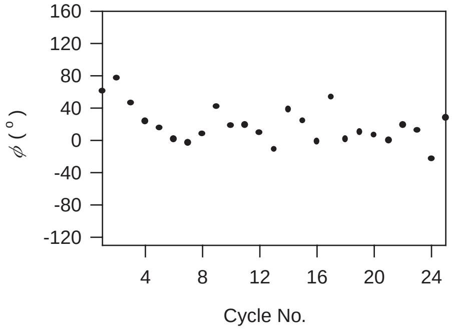

Fig. 6. Phase angles versus cycle number for $f_{vac} = 0.12$ and $\zeta = 0.02$ for Re = 8000.

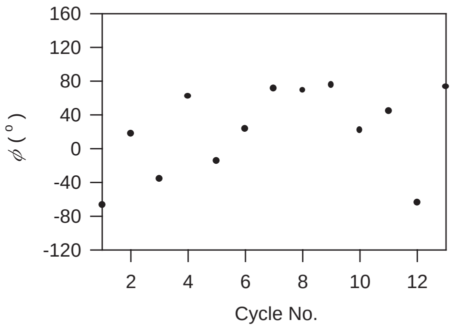

Fig. 7. Phase angles versus averaged cycle number for $f_{vac} = 0.09$ and $\zeta = 0.0$ for Re = 8000.

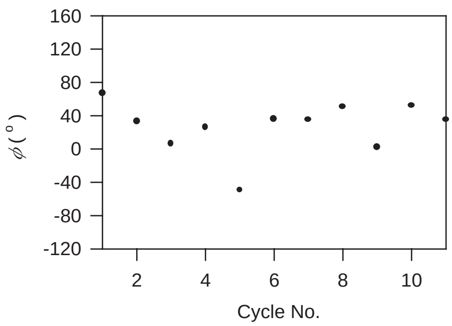

Fig. 8. Phase angles versus averaged cycle number for $f_{vac} = 0.12$ and $\zeta = 0.02$ for Re = 8000.

addition to the unknown number of frequencies the signal carries. On the other hand, a random signal does not have the characteristics of an irregular signal.

When two essentially irregular signals, such as force and displacement for a self-excited oscillation with amplitude and period both variable, are compared to find their phase relationship, there are several approaches that can be taken to obtain the phase angles. One approach is to analyze every cycle, determining the phase angle for each cycle. A second approach is to take a number of consecutive cycles, say 10, average them, and then find an average phase angle for this average cycle. This second approach was suggested by Sarpkaya (2003) and represents a means to determine an average value over a large number of cycles.

Figs. 1 and 2 show the C_L and A/D behaviors for two different self-excited results, one with material damping and one without, from calculations at or near synchronization done by Al Jamal and Dalton (2004). The average phase-angle values are defined in terms of the lag that the displacement results have at each zero upcrossing of the force coefficient curve. Figs. 3–6 show clearly that the phase angles are not constant. Figs. 3 and 6 represent the phase angles from the results in Figs. 1 and 2, while Figs. 4 and 5 are for another set of parameters, both near synchronization, but without material damping. In fact, for this approach of analyzing every cycle, the phase angles shown in Fig. 3 ($f_{\text{vac}} = 0.09$ and $\zeta = 0.0$) range from -92° to $+82^\circ$, with no obvious trend present in the results and no obvious regions of small phase-angle values. The same lack of a trend of phase-angle variation is also found in the phase angles plotted in Figs. 4–6. There is, however, a slight difference between the results shown in Fig. 3 and those in Figs. 4–6. As the value of f_{vac} approaches the value of f_{St}, as in Figs. 4–6, there exist ranges within the plots where the phase angles are quite small, but hardly a constant value.

The second approach, constructing an average cycle for every 10 cycles of oscillation, to obtain the corresponding average phase angle between the transverse force and the cylinder oscillation, yielded results similar to those obtained for the first method of phase-angle calculation. In Figs. 7 and 8, there is again a wide range of phase angles with no discernible trend in their behavior.

Figs. 3 and 7 represent the same computational case with the phase angles determined from the two distinct means discussed above. Similarly, Figs. 6 and 8 represent the same, albeit different from Figs. 3 and 7, computational case. It is clear from these two comparisons that the phase angle variations are relatively independent of their means of determination.

An obvious observation from these results is that there is no consistent phase-angle behavior when the cylinder motion is self-excited with an irregular oscillatory response. It also follows that the standard 2S, 2P, etc. vortex patterns observed by Williamson and Roshko (1988) would not be expected in this nonsinusoidal oscillation case.

3.2. Spectral decomposition

The phase angle analysis showed that this CFD representation of VIV did not yield a constant phase angle as was found in the forced oscillation results or in self-excited VIV studies at lower Reynolds numbers. The displacement and C_L calculations do not occur at a constant frequency of oscillation. So, a natural question to ask is the following: What are the spectral distributions for the time-dependent displacement and lift coefficient?

To answer this question, we analyzed eight different cases from the results of Al Jamal and Dalton (2004), all at $\text{Re} = 8000$ and $m^* = 7.85$, and the corresponding results are shown in Table 1. The results will be discussed in order for

Table 1
Spectral results for lift and displacement

V_R	ζ	$A_{\max}$	Displacement			C_L		
			Peak mag.	Peak freq.	Range	Peak mag.	Peak freq.	Range
6.25	0	0.31	13	0.075	0.045–0.11	70, 230	0.065, 0.125	0–0.14
6.25	0.02	0.26	6.9	0.075	0.06–0.12	05, 220	0.07, 0.12	0–0.45
5.55	0	0.33	27	0.08	0.07–0.1	220, 210	0.08, 0.12	0.04–0.13
5.55	0.02	0.3	15	0.08	0.07–0.15	175, 120	0.08, 0.125	0.01–0.13
4.55	0.0	0.31	175	0.1	0.088–0.108	2900	0.96	0.08–0.105
4.55	0.02	0.25	75	0.1	0.083–0.118	1500	0.96	0.06–0.105
4.17	0.0	0.31	122	0.107	0.1–0.12	3800	0.107	0.082–0.115
4.17	0.02	0.24	34	0.107	0.1–0.12	1000	0.107	0.085–0.115

the spectral representation of displacement and C_L. Each of the cases represents a situation which occurs in the lock-on region.

From Table 1, we see that each of the displacements has a peak frequency slightly less than the natural frequency in a vacuum (f_{vac}) at each value of V_R. Each case has only one dominant displacement peak, even though there is a range of frequencies, as shown in Table 1, for which there is a nonnegligible spectral content for the displacement. We also note that the maximum amplitude of oscillation and the peak magnitude of the spectral plot decrease with the inclusion of a damping term of 0.02. The damping effect is noted to increase as V_R increases. A typical set of results for displacement is shown in Fig. 10 at $V_R = 4.55$ for both the damping and no-damping cases.

Also shown in Table 1 are the C_L results. For the lower values of V_R, $V_R = 4.17$ and 4.55, the oscillation is in the early part of the lock-on region in regard to the value of V_R. In this region, there is a dominant value of C_L magnitude and a peak frequency that is essentially the same as the displacement peak frequency at the same value of V_R. There is also a range of frequencies for which the spectral content of C_L is nonnegligible. The implication is that, in this VIV case, the lift does not occur at a constant frequency or amplitude. For the two higher values of V_R, which are near the end of the lock-on region, we note that there are two dominant frequencies in the spectral description of C_L. In both of these cases, we note that the lower frequency is essentially the same as the peak frequency for the displacement that was observed earlier to be slightly less than the value of f_{vac}. The second, and typically higher, frequency is approximately equal to the vortex shedding frequency of the nonoscillating cylinder at Re = 8000. The fact that these two frequencies have the values they do suggests that the lock-on effects are diminishing. At $V_R = 5.55$ in Fig. 9, we note that damping has not influenced the lock-on behavior; the frequency ratio, f_{St}/f_{vac}, shows the same value for both the damped and undamped cases. However, at $V_R = 6.25$, which is near the end of lock-in, Fig. 9 shows that the damped oscillation is out of the lock-on region and the undamped case is still experiencing lock-on.

Fig. 10 shows the displacement power spectrum for $V_R = 4.55$ with and without damping. The effect of damping is to spread out the spectrum over a wider range of frequencies than for the case with no damping. This can be seen by comparing Figs. 10(a) and (b), where Fig. 10(b), with damping, has a secondary peak not seen in Fig. 10(a), no damping. Note also that damping has a noticeable effect in reducing the spectrum peak value which infers a smaller oscillatory magnitude at the peak frequency.

Fig. 11 shows the C_L spectral results for $V_R = 6.25$. Note that the frequency spread for the damped case is greater than that for the undamped case at this value of V_R which is at the high end of the lock-on region. In fact, this observation is true for each of the other three values of V_R. Damping causes a greater spread of the spectral content of the lift coefficient. It is worthwhile to note that the natural shedding frequency of the nonoscillating cylinder is still preserved in the flow field even though the cylinder is experiencing lock-on behavior. This frequency preservation is obvious in the appearance of two dominant spikes in the spectral results of $V_R = 5.55$ and 6.25. However, for the cases of $V_R = 4.55$ and $V_R = 4.17$, there is one dominant spike in the spectral decomposition, as shown in Fig. 12 for $V_R = 4.55$. The appearance of one single frequency rather than two distinct frequencies can be interpreted as the closeness in value between f_{vac} and f_{St} which results in a more energy concentration at one frequency. This concentration is evident from the large values the single spike takes for these two cases.

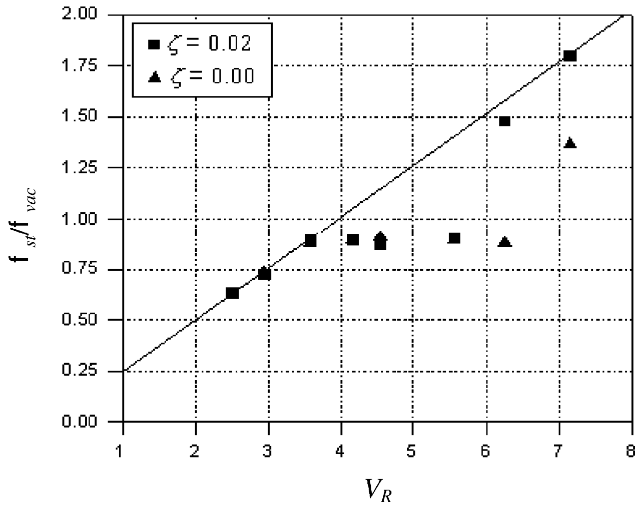

Fig. 9. Shedding frequency in the lock-on region at Re = 8000.

3.3. Complex demodulation

In addition to the previous analyses of phase angles, we have preformed a complex demodulation of the lift and displacement signals, as described by Bloomfield (1976), to determine what the time-dependency is of their phase difference. This method is based on representing a reference signal, i.e., the displacement signal, by

$$D(\tau) = R_D(\tau)\exp[\mathrm{i}(\lambda_D\tau + \varphi_D(\tau))], \quad (5)$$

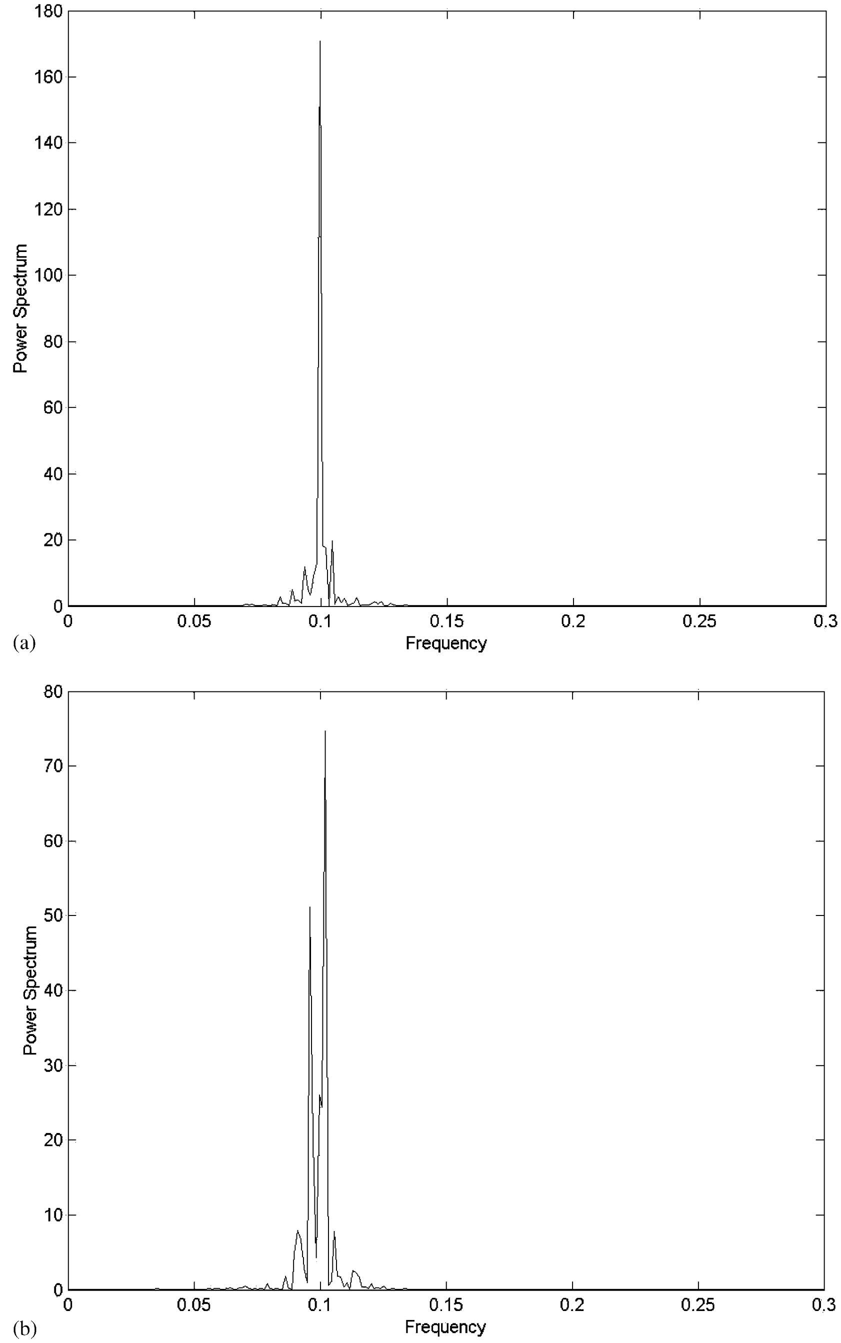

Fig. 10. Displacement spectrum at $V_R = 4.55$ ($f_{\mathrm{vac}} = 0.11$) for Re = 8000: (a) $\zeta = 0.0$ and (b) $\zeta = 0.02$.

where λ_D is the dominant frequency, $R_D(\tau) = D(\tau)\exp[i(\lambda_D\tau)]$ is the representative amplitude, and $\varphi_D(\tau)$ is the phase angle of the reference signal and can be computed from $\exp[i(\varphi_D(\tau))] = D(\tau)/R_D(\tau)$. The same type of representation is applied to the lift signal. The difference in these two phase angles yields the difference in phase between the lift and the displacement.

Fig. 13 shows the time variation of the phase difference between the forcing signal ($C_L(\tau)$) and the displacement signal ($y(\tau)/D$) for $f_{vac} = 0.08$ with and without damping. The figure shows part of the demodulation signal because the complete signal is too dense for the phase difference behavior to be observed clearly. It is noticed that the phase

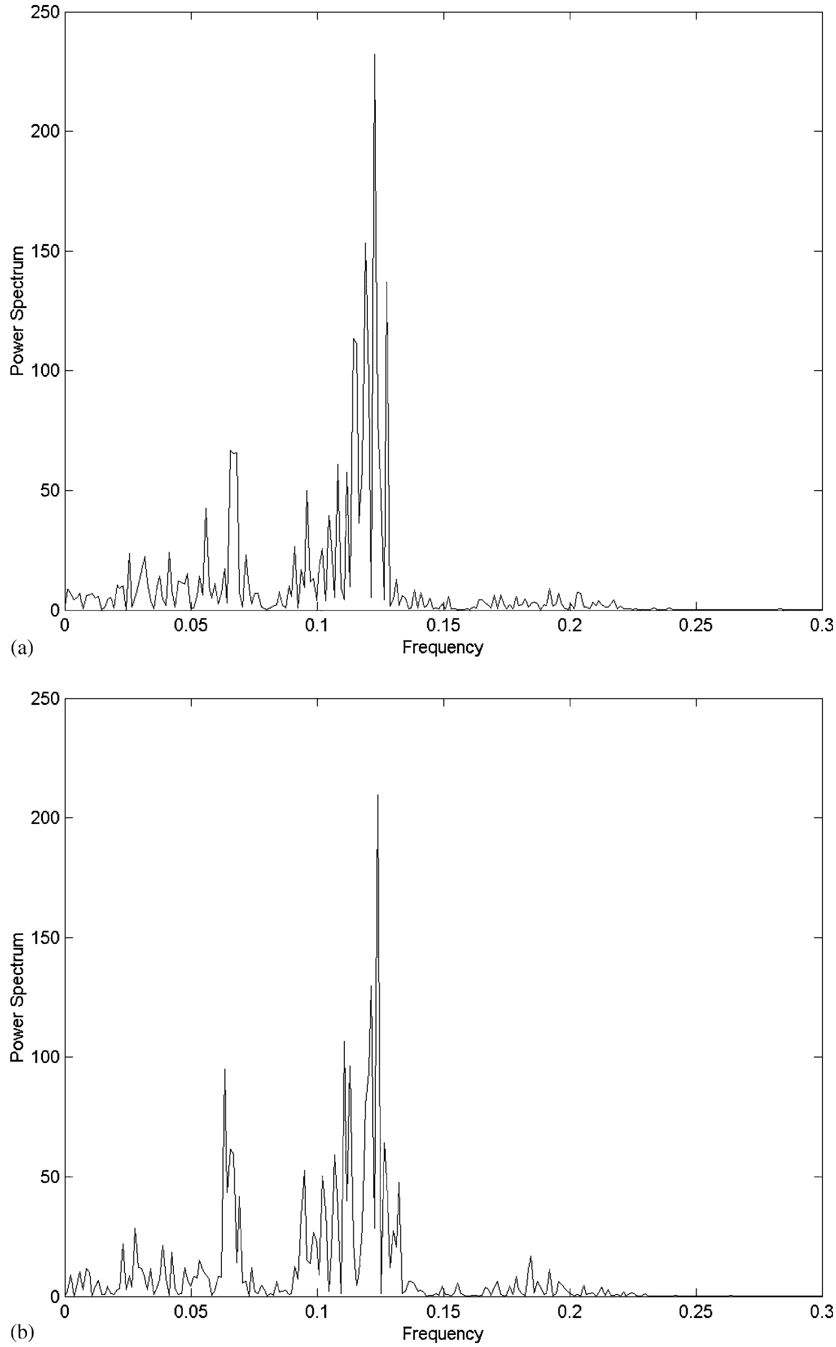

Fig. 11. Lift spectrum at $V_R = 6.25$ ($f_{vac} = 0.08$) for Re = 8000: (a) $\zeta = 0.0$ and (b) $\zeta = 0.02$.

difference takes on values of π, 0 and $-\pi$ in an irregular manner. The actual value of the phase angle is lost in this complex demodulation. The values of π, 0 and $-\pi$ simply imply that the phase angle is positive, zero, or negative, respectively. This means that the phase difference between the forcing function and the responsive displacement is continuously changing between positive and negative values. This irregular switching can be related to the irregular time-variation in vortex shedding while the cylinder is vibrating and yields, consequently, to an irregular forcing function.

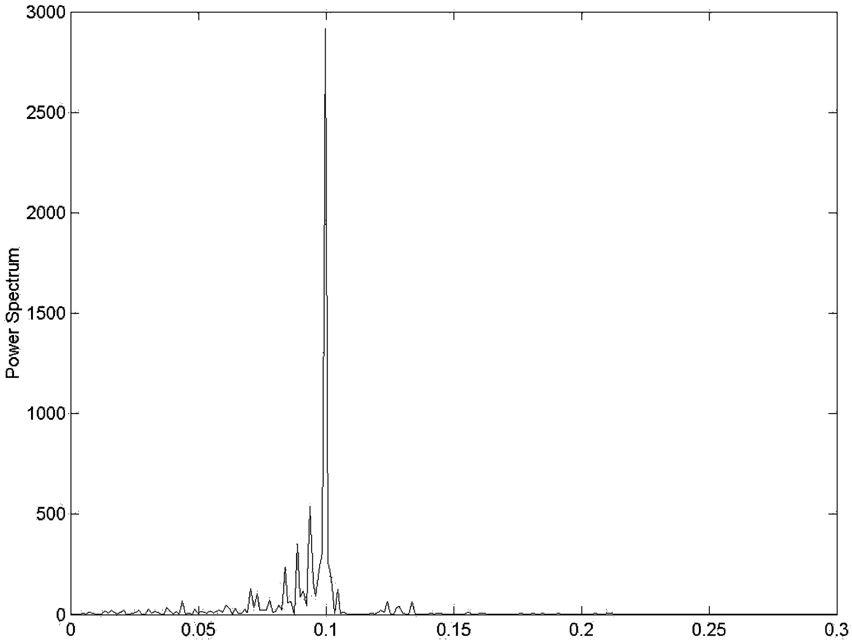

(a)

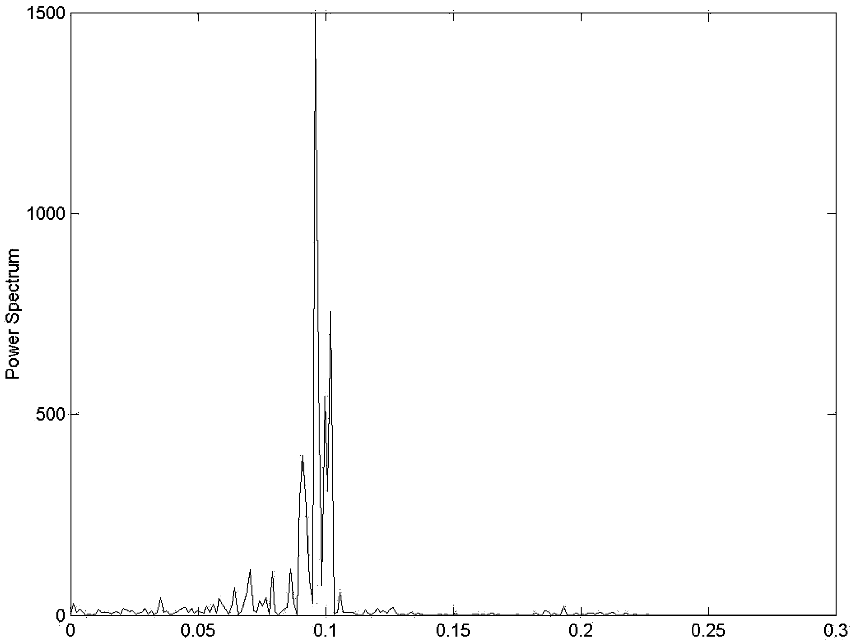

(b)

Fig. 12. Lift spectrum at $V_R = 4.55$ ($f_{\mathrm{vac}} = 0.11$) for Re = 8000: (a) $\zeta = 0.0$ and (b) $\zeta = 0.02$.

In Fig. 14, the phase difference is calculated over nine cycles for $f_{\mathrm{vac}} = 0.09$ and $\zeta = 0.02$. In Fig. 14(b), the calculation is done with a cycle-forward shift from what is shown in Fig. 14(a). The same phase difference behavior is observed. These observations support the results shown in Section 3.2, i.e., VIV, for the conditions used herein, occurs with unexpected phase angle variations due to the irregular forcing nature of the complicated flow patterns (Figs. 14(c), 14(d)).

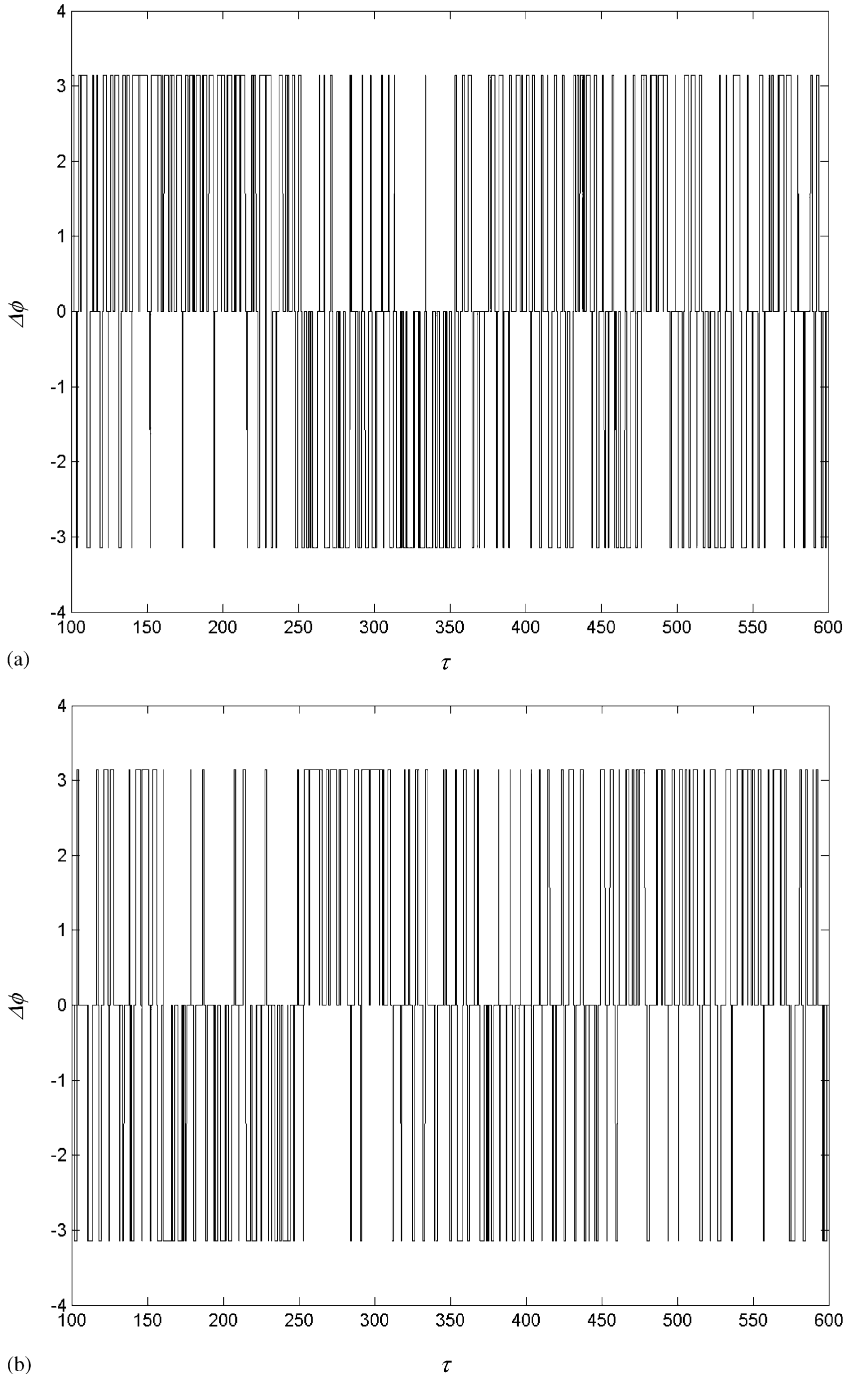

Fig. 13. Time-variation phase-difference at $V_R = 6.25$ ($f_{\mathrm{vac}} = 0.08$) for Re $= 8000$: (a) $\zeta = 0.02$ and (b) $\zeta = 0.0$.

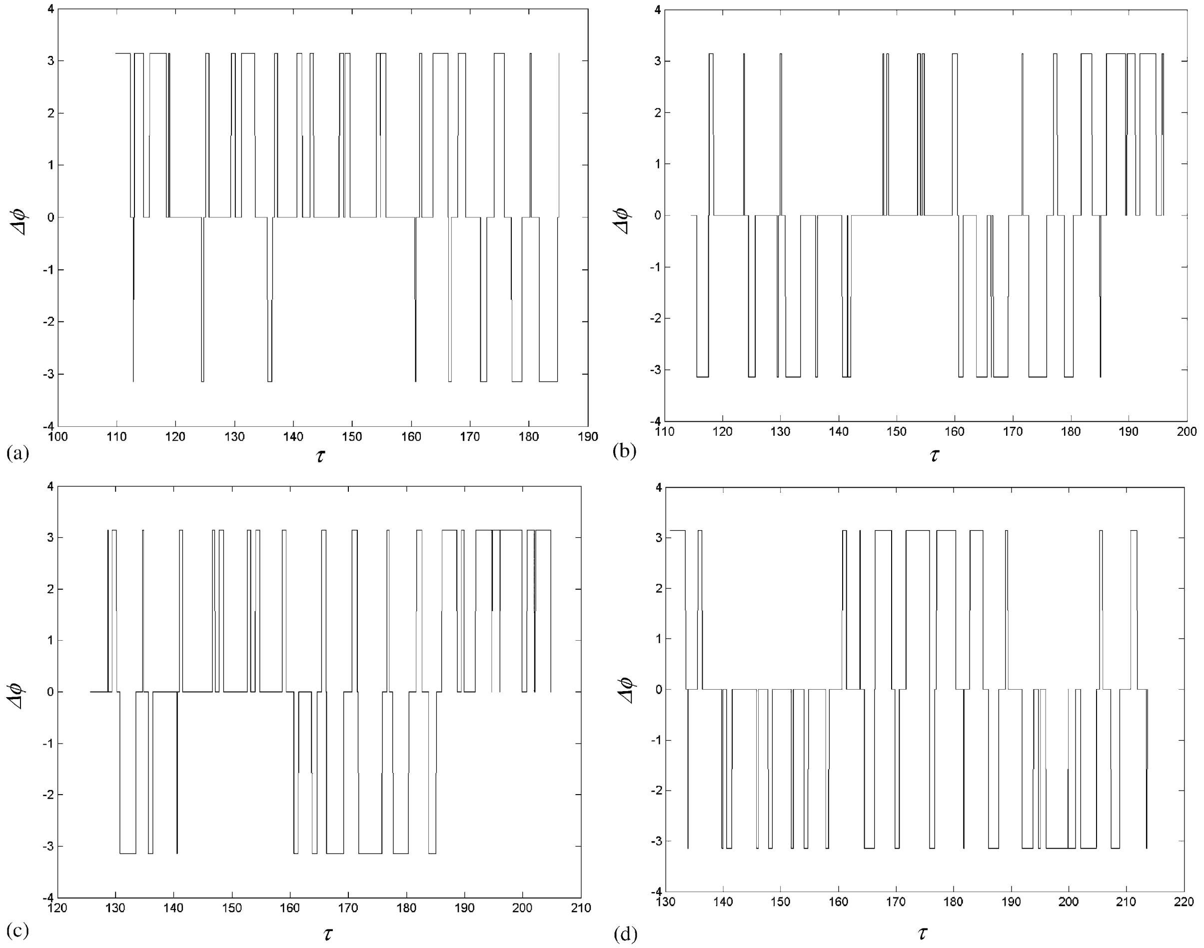

Fig. 14. (a) Time-variation phase-difference over nine oscillatory cycles at $V_R = 5.56$ ($f_{vac} = 0.09$) and $\zeta = 0.02$ for Re = 8000. (b) Time-variation phase-difference over nine oscillatory cycles (one cycle forward from (a)) at $V_R = 5.56$ ($f_{vac} = 0.09$) and $\zeta = 0.02$ for Re = 8000. (c) Time-variation phase-difference over nine oscillatory cycles (one cycle forward from (b)) at $V_R = 5.56$ ($f_{vac} = 0.09$) and $\zeta = 0.02$ for Re = 8000. (d) Time-variation phase-difference over nine oscillatory cycles (one cycle forward from (c)) at $V_R = 5.56$ ($f_{vac} = 0.09$) and $\zeta = 0.02$ for Re = 8000.

4. Conclusions

When a self-excited transverse oscillation of a cylinder occurs with an irregular response behavior, there is no phase-angle correlation between the forcing function and the cylinder oscillation at the intermediate value of Reynolds number analyzed in this study. This observation is based on both a spectral analysis and a complex demodulation of the LES calculations of Al Jamal and Dalton and by several other investigators as mentioned earlier. This result is in contrast to what is frequently found when the cylinder motion is from a forced sinusoidal oscillation or when the self-excited response is sinusoidal. In the case of constant oscillation amplitude, the wake vortex patterns are repeatable and the established shedding patterns, 2S, 2P, P + S, etc., can occur. In the self-excited case with an irregular response, the cylinder oscillation is not sustained sufficiently for the expected vortex-mode patterns, from the sinusoidal oscillations, to develop or be established. The absence of the expected vortex-mode patterns is responsible for the lack of a consistent phase angle between the forcing function and the cylinder response. This complex problem requires further study before all of the questions posed earlier can be answered.

Acknowledgements

We are grateful to Dexter Hill of NEC Systems, Inc. for providing computer time on the SX4 machine at the NEC facility in The Woodlands, TX. We are grateful to Turgut Sarpkaya and Jeff Zhang for several helpful discussions. Ajay Rao and Viju Rao both helped with the spectral calculations.

References

Al Jamal, H., Dalton, C., 2004. Vortex-induced vibrations using large eddy simulation at a moderate Reynolds number. Journal of Fluids and Structures 19, 73–92.

Bishop, R.E.D., Hassan, A.Y., 1964. The lift and drag forces in a circular cylinder in a flowing fluid. Proceedings of the Royal Society of London A 277, 32–48.

Blackburn, H.M., Henderson, R.D., 1999. A study of two-dimensional flow past an oscillating cylinder. Journal of Fluid Mechanics 385, 255–286.

Blackburn, H.M., Govardhan, R.N., Williamson, C.H.K., 2001. A complementary numerical and physical investigation of vortex-induced vibration. Journal of Fluids and Structures 15, 481–488.

Bloomfield, P., 1976. Fourier Analysis of Time Signals: An Introduction. Wiley, New York.

Brika, D., Laneville, A., 1993. Vortex-induced vibrations of a long flexible cylinder. Journal of Fluid Mechanics 250, 451–508.

Carberry, J., Sheridan, J., Rockwell, D., 2001. Forces and wake modes of an oscillating cylinder. Journal of Fluids and Structures 15, 523–532.

Dong, S., Karniadakis, G.E., 2004. DNS of flow past a stationary and oscillating rigid cylinder at $Re = 10{,}000$. Flow-induced Vibration Conference, FIV 2004, Paris (See also the updated paper in this issue of JFS).

Evangelinos, C., Karniadakis, G.E., 1999. Dynamics and flow structures in the turbulent wake of rigid and flexible cylinders subject to vortex-induced vibration. Journal of Fluid Mechanics 400, 91–124.

Feng, C.C., 1968. The measurement of vortex-induced effects in flow past stationary and oscillating circular and D-section cylinders. M.A.Sc. Thesis, The University of British Columbia, Vancouver, Canada.

Govardhan, R., Williamson, C.H.K., 2000. Modes of vortex formation and frequency response of a freely vibrating cylinder. Journal of Fluid Mechanics 420, 85–130.

Gu, W., Chyu, C., Rockwell, D., 1994. Timing of vortex shedding from an oscillating cylinder. Physics of Fluids 6, 3677–3682.

Guilmineau, E., Queutey, P., 2002. A numerical simulations of vortex shedding from an oscillating circular cylinder. Journal of Fluids and Structures 16, 773–794.

Guilmineau, E., Queutey, P., 2004. Numerical simulation of vortex-induced vibration of a circular cylinder with low mass damping. Journal of Fluids and Structures 19, 449–466.

Khalak, A., Williamson, C.H.K., 1999. Motions, forces, and mode transitions in vortex-induced vibrations at low mass damping. Journal of Fluids and Structures 13, 813–851.

Lienhard, J.H., Liu, L.W., 1967. Locked-in vortex shedding behind oscillating circular cylinders, with application to transmission lines. ASME Paper 67-FE-24.

Lu, X., Dalton, C., 1996. Calculation of the timing of vortex formation from an oscillating circular cylinder. Journal of Fluids and Structures 10, 527–541.

Lucor, D., Foo, J., Karniadakis, G.E., 2004. Vortex mode selection of a rigid cylinder subject to VIV at low mass-damping. Flow-induced Vibration Conference, FIV 2004, Paris (See also updated paper in this issue of JFS).

Moe, G., Wu, Z.J., 1990. The lift force on a cylinder vibrating in a current. Journal of Offshore Mechanics and Arctic Engineering 112, 297–303.

Moe, G., Holden, K., Yttervoll, P.O., 1994. Motion of spring-supported cylinders in subcritical and critical water flows. Proceedings of the Fourth International Offshore and Polar Engineering Conference, Osaka, Japan.

Ongoren, A., Rockwell, D., 1988. Flow structure from an oscillating cylinder, Part 1. Mechanisms of phase shift and recovery in the near wake. Journal of Fluid Mechanics 191, 197–223.

Sarpkaya, T., 1978. Fluid forces on oscillating cylinders. ASCE Journal of Waterway, Port, Coastal, and Ocean Division 104, 275–290.

Sarpkaya, T., 1995. Hydrodynamic damping, flow-induced oscillation, and biharmonic response. ASME Journal of Offshore Mechanics and Arctic Engineering 117, 232–238.

Sarpkaya, T., 2003. Naval Postgraduate School, Monterey, CA. Personal Communication.

Sarpkaya, T., 2004. A critical review of the intrinsic nature of vortex-induced vibrations. Journal of Fluids and Structures 19, 389–447.

Tutar, M., Holdo, A.E., 2000. Large eddy simulation of a smooth circular cylinder oscillating normal to a uniform flow. ASME Journal of Fluids Engineering 122, 694–702.

Williamson, C.H.K., Roshko, A., 1988. Vortex formation in the wake of an oscillating cylinder. Journal of Fluids and Structures 2, 355–381.

Zdravkovich, M.M., 1982. Modification of vortex shedding in the synchronization range. ASME Journal of Fluids Engineering 104, 513–517.